Linköping University Post Print

Pressure enhancement of the isostructural cubic decomposition in $Ti_{1-x}Al_xN$



N.B.: When citing this work, cite the original article.

Original Publication:

Björn Alling, Magnus Odén, Lars Hultman and Igor Abrikosov, Pressure enhancement of the isostructural cubic decomposition in Ti_{1-x}Al_xN, 2009, Applied Physics Letters, (95), 181906. http://dx.doi.org/10.1063/1.3256196

Copyright: American Institute of Physics

http://www.aip.org/

Postprint available at: Linköping University Electronic Press http://urn.kb.se/resolve?urn=urn:nbn:se:liu:diva-51569

Pressure enhancement of the isostructural cubic decomposition in $Ti_{1-x}AI_xN$

B. Alling, ^{a)} M. Odén, L. Hultman, and I. A. Abrikosov *Department of Physics, Chemistry, and Biology (IFM), Linköping University, SE-581 83 Linköping, Sweden* (Received 28 September 2009; accepted 7 October 2009; published online 2 November 2009)

The influence of pressure on the phase stabilities of $Ti_{1-x}Al_xN$ solid solutions has been studied using first principles calculations. We find that the application of hydrostatic pressure enhances the tendency for isostructural decomposition, including spinodal decomposition. The effect originates in the gradual pressure stabilization of cubic AlN with respect to the wurtzite structure and an increased isostructural cubic mixing enthalpy with increased pressure. The influence is sufficiently strong in the composition-temperature interval corresponding to a shoulder of the spinodal line that it could impact the stability of the material at pressures achievable in the tool-work piece contact during cutting operations. © 2009 American Institute of Physics. [doi:10.1063/1.3256196]

TiAlN is widely used as hard protective coating in cutting tool applications. The cubic B1 Ti_{1-x}Al_xN solid solutions have been found to have superior properties as compared to TiN coatings especially in high temperature applications. One main reason behind the success is the retained or even increased hardness of the material at temperatures up to around 1273 K.²⁻⁴ This age hardening was explained through a mechanism of coherent isostructural decomposition such as spinodal decomposition of the metastable solid solutions into cubic Al- and Ti-enriched $Ti_{1-x}Al_xN$ domains.^{2,5,6} The presence of such decomposition behavior was later confirmed theoretically by means of firstprinciples calculations revealing an electronic structure origin as the main driving force for decomposition. Since then several subsequent studies have highlighted different aspects of importance for the understanding of this materials system, such as the influence of nitrogen off-stoichiometry,8 the importance of an accurate modeling of the disordered distribution of Ti and Al atoms on the metal sublattice, and domain growth behavior. 10 Although the effect of temperature on the phase stability and performance of Ti_{1-x}Al_xN coatings has attracted much attention, the effect of pressure has this far been neglected. This is so even though it is known that application of high pressure enhances opportunities for materials design, and that the applied force of a cutting tool against the work piece, together with the minimal contact area, gives rise to stress or pressure levels of several GPa at the cutting edge.11

In this work, we model the pressure effect by considering the impact of hydrostatic pressure on the phase stabilities of the $\mathrm{Ti}_{1-x}\mathrm{Al}_x\mathrm{N}$ system theoretically using first-principles density functional theory. We model the solid solutions in the cubic rock salt and hexagonal wurtzite structures using the special quasirandom structures method 7,12 which allows us to directly monitor the effect of pressure on the energetics and thermodynamics of the solution phases including the effect of local lattice relaxations. The cubic system was considered over the entire concentration range while the hexagonal system was studied for $0.75 \le x \le 1.00$. All calculations were performed using the projector augmented wave method 13 as implemented in the Vienna *ab initio* simulation package.

The exchange-correlation effects were modeled using the generalized gradient approximation. ¹⁶ The equation of states for all systems was derived from a fitting of a modified Morse function ¹⁷ to the calculated energy values.

The starting point of our analysis is the mixing enthalpies of the cubic and hexagonal solid solutions as a function of pressure and composition. The panel (a) of Fig. 1 shows the mixing enthalpies with respect to cubic TiN and hexagonal AlN at ambient pressure, as well as at 5 and 10 GPa. The gradual stabilization of the cubic phase in the AlN rich region by pressure is clearly seen from a decrease in the mixing enthalpy. The calculated equilibrium transition pressure of pure AlN at 0 K is 12.9 GPa which is identical to the calculated value in Ref. 18. This is in line with the experimental findings in Ref. 19 that the structural transition starts at 14-16.5 GPa and that the rock salt structure is metastable at ambient conditions. The crossing point of the enthalpies of the cubic and hexagonal phases shifts from x=0.71 at 0 GPa (Ref. 20) to x=0.83 at 5 GPa and x=0.94 at 10 GPa. This

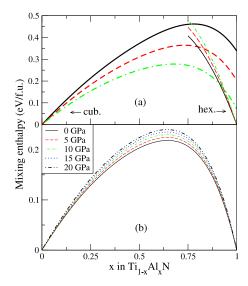


FIG. 1. (Color online) (a) Mixing enthalpy of cubic rock salt (thick lines) and hexagonal wurtzite (thin lines) $Ti_{1-x}Al_xN$ as a function of Al content x, for different pressures between p=0 GPa and p=10 GPa, relative to cubic TiN and hexagonal AlN. (b) Isostructural cubic mixing enthalpy of $Ti_{1-x}Al_xN$ as a function of pressure.

^{a)}Electronic mail: bjoal@ifm.liu.se.

FIG. 2. (Color online) Mean field phase-diagram of the isostructural cubic $Ti_{1-x}AI_xN$ system as a function of pressures from 0 to 20 GPa. The binodal lines are shown with thick lines while the spinodal is shown with thin lines. The inset shows an enlarged zoom in of the region where the effect of pressure on the spinodal is most pronounced.

finding indicates that cubic AlN-rich domains are less likely to transform to the undesired hexagonal structure during for example cutting operations where the TiAlN coating is exposed to a combination of heat and pressure, compared to ambient pressure anneals, even if the same time and temperature are reached.

Panel (b) of Fig. 1 shows the cubic isostructural mixing enthalpies calculated with respect to c-TiN and c-AlN as a function of pressure. The mixing enthalpy curves show a clear asymmetry with the maxima shifted to the AlN-rich side. This was studied in detail in Ref. 7 and the explanation was found to be an unfavorable localization of Ti d-states at the Fermi level in AlN-rich samples. The effect of pressure on the isostructural mixing enthalpy is positive in contrast to the nonisostructural case. However the change is small, the maximum value is increased from 0.22 eV/f.u. at 0 GPa to 0.24 eV/f.u. at 20 GPa.

Based on these mixing enthalpies derived at different pressures, we construct the isostructural phase diagrams in Fig. 2 using the pressure independent mean field contribution for configurational entropy and temperature effects. The common tangent construction is used to derive the binodal lines while the condition $(\partial^2 G/\partial x^2)=0$ is used to define the spinodal line. As in Ref. 7, a fifth order polynomial fit to the calculated enthalpies is used in order to stabilize the numerical differentiation. The cubic isostructural phase diagram is of relevance when analyzing possible coherent decomposition, including spinodal decomposition, from a metastable cubic solid solution formed during thin film growth of $Ti_{1-x}Al_xN$ with x < 0.70. Furthermore, at pressures above the transition from wurtzite to rock salt AlN, the system is actually isostructural in equilibrium. The effect of small pressures on the average appearance of the phase diagram is not large. This is in line with textbook formulations that the effect of pressure on phase diagrams is expected to be small. However, due to the asymmetry of the mixing enthalpies, the spinodal lines show a distinct shoulder at compositions just below x=0.50. At this specific composition and temperature interval also relatively small pressures can substantially increase the spinodal region at a given temperature. The inset in Fig. 2 shows this effect. For instance, going from ambient pressure to 5 GPa extends the spinodal region on the Ti-rich side from x=0.36 to x=0.32 at 2250 K. Here one should keep in mind that the mean field approximation for temperature effects is a qualitative method and that critical temperatures are typically overestimated due to the neglect of short range order or clustering effects. However, the qualitative shape of the phase diagram should be well described since its physical origin comes from the electronic structure variation with alloy composition, as shown in Refs. 7 and 9.

This means that the tendency for spinodal decomposition, shown to exist in ambient pressure thermal annealing experiments, 5,21 should actually be even more pronounced under real cutting tools operations due to the presence of compressive stress in the critical region of the coating.

To understand the origin of the pressure effects on the mixing enthalpies and the phase diagram we note that the pressure derivative of the Gibb's free energy at fixed temperature

$$\left(\frac{\partial G}{\partial p}\right)_T = V. \tag{1}$$

Analyzing instead the free energy of mixing

$$\Delta G = G_{\text{Ti}_{1-x}\text{Al}_x\text{N}} - (1-x)G_{\text{TiN}} - xG_{\text{AlN}}, \tag{2}$$

we find

$$\left(\frac{\partial \Delta G}{\partial p}\right)_T = \Delta V \tag{3}$$

where

$$\Delta V = V_{\text{Ti}_{1-x}\text{Al}_x\text{N}} - (1-x)V_{\text{TiN}} - xV_{\text{AlN}}.$$
 (4)

This is the difference of the volume of the solid solution compared to a linear interpolation between the volumes of the components. In the nonisostructural case it is obvious that the pressure derivative of the free energy of the cubic solid solutions will be negative since its volume is compared with the mixture of TiN and the large volume h-AlN and thus $\Delta V < 0$. In the isostructural case on the other hand the trend is reversed. It has been established that there is a positive deviation from Vegard's rule in this system⁷ as well as in the related systems $Cr_{1-x}Al_xN$, $Sc_{1-x}Al_xN$, and $Hf_{1-x}Al_xN$. Such a behavior results in $\Delta V > 0$ at ambient pressure, and thus it is directly related to the increasing tendency for decomposition, at least at relatively low pressures.

Since ΔV in Eq. (4) is pressure dependent the trends could change with increasing pressure. In Fig. 3 the calculated volumes of the cubic solid solutions are plotted for 0, 10, and 20 GPa. The system exhibits $\Delta V(p) > 0$ for all compositions and pressures considered. However a small gradual decrease in ΔV is present indicating a possible saturation of the predicted impact on phase stability at high pressures.

Since Eqs. (1)–(4) are not limited to the mean field approximation, we conclude that the only term effecting $(\partial G/\partial p)_T$ neglected in this work is the change in volume with temperature, i.e., thermal expansion. Further more, an exact derivation of $(\partial \Delta G/\partial p)_T$ would only be different from our approximation if there is a deviation from a Vegard's rule type dependence of the thermal expansion in this system.

In conclusion, we have calculated mixing enthalpies of the TiAlN system as a function of pressure and constructed the binodal and spinodal lines of the cubic isostructural

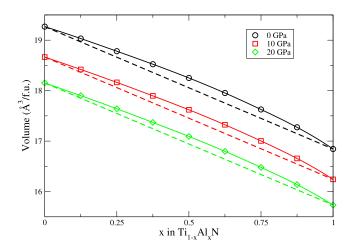


FIG. 3. (Color online) Calculated equilibrium volumes of the cubic $Ti_{1-x}Al_xN$ system as a function of AlN content and pressure. The symbols are the calculated values, the dashed lines corresponds the volumes predicted from Vegard's rule. The solid lines are interpolations to guide the eye.

phase diagram using the mean field approximation. We find that even relatively small pressures promote coherent isostructural decomposition. This is explained through the suppression of the formation of the incoherent hexagonal phases as well as an increased tendency for spinodal decomposition into cubic AlN and TiN rich regions upon hydrostatic compression. Both effects can be understood from the deviations of the solid solution volume from Vegard's rule. We conclude that the beneficial age hardening mechanism observed in $\mathrm{Ti}_{1-x}\mathrm{Al}_x\mathrm{N}$ coatings in ambient pressure, thermal annealing experiments should be even more pronounced in real cutting operations due to pressure effects. These qualitative observations motivate further experimental and theoretical investigations.

Financial support from the Swedish Research Council (VR), the Swedish Foundation for Strategic Research (SSF),

and the Göran Gustafsson Foundation for Research in Natural Sciences and Medicine is gratefully acknowledged. Most of the simulations were carried out at the Swedish National Infrastructure for Computing (SNIC).

¹O. Knotek, M. Böhmer, and T. Leyendecker, J. Vac. Sci. Technol. A 4, 2695 (1986).

²P. H. Mayrhofer, A. Hörling, L. Karlsson, J. Sjölén, T. Larsson, C. Mitterer, and L. Hultman, Appl. Phys. Lett. 83, 2049 (2003).

³A. E. Santana, A. Karimi, V. H. Derflinger, and A. Schutze, Tribol. Lett. **17**, 689 (2004).

⁴A. Hörling, L. Hultman, M. Odén, J. Sjölen, and L. Karlsson, Surf. Coat. Technol. 191, 384 (2005).

⁵A. Hörling, L. Hultman, M. Oden, J. Sjölen, and L. Karlsson, J. Vac. Sci. Technol. A **20**, 1815 (2002).

⁶A. Knutsson, M. P. Johansson, P. O. A. Persson, L. Hultman, and M. Odén, Appl. Phys. Lett. **93**, 143110 (2008).

⁷B. Alling, A. V. Ruban, A. Karimi, O. E. Peil, S. I. Simak, L. Hultman, and I. A. Abrikosov, Phys. Rev. B **75**, 045123 (2007).

⁸B. Alling, A. Karimi, L. Hultman, and I. A. Abrikosov, Appl. Phys. Lett. **92**, 071903 (2008).

⁹B. Alling, A. Karimi, and I. A. Abrikosov, Surf. Coat. Technol. **203**, 883 (2008).

¹⁰M. Odén, L. Rogström, A. Knutsson, M. R. Terner, P. Hedström, J. Almer, and J. Ilavsky, Appl. Phys. Lett. **94**, 053114 (2009).

¹¹R. M'Saoubi and S. Ruppi, CIRP Ann. **58**, 57 (2009).

¹²A. Zunger, S. H. Wei, L. G. Ferreira, and J. E. Bernard, Phys. Rev. Lett. 65, 353 (1990).

¹³P. E. Blöchl, Phys. Rev. B **50**, 17953 (1994).

¹⁴G. Kresse and J. Hafner, Phys. Rev. B 48, 13115 (1993).

¹⁵G. Kresse and D. Joubert, Phys. Rev. B **59**, 1758 (1999).

¹⁶J. P. Perdew, K. Burke, and M. Ernzerhof, Phys. Rev. Lett. 77, 3865 (1996)

¹⁷V. L. Moruzzi, J. F. Janak, and K. Schwarz, Phys. Rev. B **37**, 790 (1988).

¹⁸P. Van Camp, V. E. V. Doren, and J. T. Devreese, Phys. Rev. B 44, 9056 (1991).

¹⁹H. Vollstädt, E. Ito, M. Akaishi, S. Akimoto, and O. Fukunaga, Proc. Jpn. Acad., Ser. B: Phys. Biol. Sci. 66, 7 (1990); Q. Xia, H. Xia, and A. L. Ruoff, J. Appl. Phys. 73, 8198 (1993).

²⁰B. Alling, Ph.D. thesis, École Polytechnique Fédérale de Lausanne, 2009.

²¹R. Rachbauer, E. Stergar, S. Massl, M. Moser, and P. H. Mayrhofer, Scr. Mater. 61, 725 (2009).